Fuel 290 (2021) 120029

Contents lists available at ScienceDirect

Fuel

journal homepage: www.elsevier.com/locate/fuel

Full Length Article

Impact of equilibration time lag between matrix and fractures on the evolution of coal permeability

Mingyao Wei [a,*], Jishan Liu [b], Derek Elsworth [c], Yingke Liu [d], Jie Zeng [b], Zhihong He [e]

[a] National and Local Joint Engineering Laboratory of Internet Application Technology on Mine, IoT Perception Mine Research Center, China University of Mining and Technology, Xuzhou, Jiangsu 221116, China
[b] School of Engineering, The University of Western Australia, 35 Stirling Highway, Perth, WA 6009, Australia
[c] Department of Energy and Mineral Engineering, G3 Center and Energy Institute, The Pennsylvania State University, University Park, PA16802, USA
[d] National Engineering Research Center for Coal Mine Gas Control, China University of Mining and Technology, Xuzhou, Jiangsu 11 221116, China
[e] Xishan Coal Electricity Group Co., Ltd, Taiyuan, Shanxi 030024, China

ARTICLE INFO

Keywords:
Dual-permeability model
Gas adsorption
Coal permeability
Equilibration time lag
Reservoir simulation

ABSTRACT

In conventional dual porosity models, the interactions between matrix and fractures are normally characterized through two equilibrium systems within the same REV (representative elementary volume). This pseudo-steady approach cannot capture the true impact of the non-equilibrium period within each system since it ignores the true transient nature of the fracture-matrix interaction. In this study, a conventional dual porosity model is extended to include the impact of equilibration time lag between matrix and fractures caused by their contrasting properties. To incorporate this important mechanism, the matrix REV is divided into two sub-REVs by using the MINC concept (Multiple Interacting Continua). The time lag effect is defined as a function of the difference between the strain in the matrix REV and that in the sub-matrix REV, and incorporated into a coal permeability model. Consequently, the coal permeability evolves also from initial to final equilibrium. Conventional dual porosity/permeability models represent two end points (initial and final equilibrium) while this new permeability model represents the evolution of coal permeability between these two end points. The model is verified against experimental observations of the evolution of coal permeability under a constant effective stress that extend for more than 80 days. If effective stress remains unchanged, conventional permeability models predict no permeability changes while our new model predicts that coal permeability evolves as a function of time from initial to ultimate equilibrium. Our results suggest that the impact of matrix strain variations on the evolution of coal permeability is significant and should not be ignored.

1. Introduction

Coalbed methane (CBM) reservoirs are one of a variety of unconventional reservoirs with extremely low permeability. Coal is a typical dual porosity medium that consists of matrix and microfractures [1]. Fractures exert a significant impact on the gas flow capacity while the matrix blocks hold the majority of the reservoir storage capacity. The long-term gas extraction from coal seams involves multiple processes, such as gas desorption, desorption shrinkage and stress transfer. Therefore, a full understanding of coupled multiple processes in the combined matrix-fracture systems is critical for the efficient exploitation of coalbed methane.

Typically, the coal structure is conceptualized using a dual porosity model [2] to replicate the nature of the pore structure and hierarchy. Dual-porosity/dual permeability models are the most common in modeling naturally fractured reservoirs in commercial CBM simulators. According to the dual-porosity model, the mass transfer between fractures and matrix blocks is represented by sink/source terms [3,4]. The basic assumption of pseudo-steady state for dual-porosity models limits their applicability [5-7]. Compared to conventional reservoirs, gas production in low-permeability coal reservoirs is driven by highly nonlinear flow [8]. Thus, the classic dual-porosity model may not be applicable in a coal gas reservoir simulation as transient flow may be long-lasting [9]. The Multiple Interacting Continua (MINC) method [6] improves the transient flow simulation. In this, the matrix blocks are discretized into a sequence of nested volume elements, which are defined on the basis of distance from the fractures. This concept is able to describe gradients of pressures, temperatures, or concentrations near

* Corresponding author.
E-mail address: cumtwmy@sina.com (M. Wei).

https://doi.org/10.1016/j.fuel.2020.120029
Received 9 December 2019; Received in revised form 26 November 2020; Accepted 15 December 2020
Available online 30 December 2020

matrix surface and inside the matrix by further subdividing individual matrix blocks into one or multidimensional strings of nested meshes [10]. Another sub-domain method [11] divides the matrix blocks vertically to a number of stacked layers, and this may also accommodate both imbibition and gravity-driven displacements [12]. Sub-gridding techniques may also be applied which are constructed numerically by using *iso*-pressure surfaces of fine grid pressure solution [13] with Schwarz–Christoffel conformal mapping approaches also used [9]. Although the flow behavior inside matrix blocks can be modeled and accurately simulated using MINC method, the grid refinement of the matrix increases the computational cost, and it may not be suitable for large scale simulation of CBM extraction.

Another assumption of dual-porosity models is that the matrix block geometry and properties are uniform within each simulation cell. State variables such as gas pressure and effective stress are also assumed to be distributed equally within the matrix block [14]. These assumptions may not be applicable for unconventional reservoirs. Because of the extreme low-permeability, the flow in the matrix stabilizes only after a very long production time. Since the pressure gradient drives the gas flow from the matrix to the fracture, a differential gas pressure must exist within the matrix block during the entire period that gas production continues. Because of this differential gas pressure in the matrix, the distribution of effective stress must also be non-uniform. Hence, the classic dual-porosity model is not able to capture the spatial variation of deformation in the matrix block.

Permeability evolution within fractured coal is influenced by many factors, such as effective stress, and gas adsorption/desorption [15-18]. It is generally accepted that the fracture volume is strongly affected by coal matrix swelling [19-23]. Pang et al. [24] experimentally studied the impact of adsorption on shale gas transport in organic nanopores. Wu et al. [25] experimentally studied coupled effects of effective stress and CO_2 sorption on matrix permeability. These studies have shown that the interaction of different mechanisms plays a critical role in permeability evolution. It is shown that the pore volume in a fractured porous medium changes not only with boundary stress and pore pressure, but also with mechanical matrix-fracture interaction [26]. The internal structure is also affected by adsorption swelling in the matrix due to the irregular distribution of fractures. The pressure difference between the pore regions can contribute to changes in the respective pore volumes. Liu and Rutqvist [20] introduced a coefficient to describe the influence of sorption-induced matrix strain on the fracture width. Zhou et al. [19] built a permeability model to investigate the change of fracture width related to the matrix block deformation. These models used a fixed factor to present the part of matrix deformation affecting fracture aperture. However, these models fail to capture the feature that the effect of matrix deformation will vanish when gas pressure reaches an equilibrium state. Zhang et al. [27] introduced an overlapping approach to characterize the local deformation compatibility between the matrix and the fracture. The interaction between fracture and matrix is through mass exchange in the overlapping approach, with interlocking effects between fracture and matrix neglected. Wei et al. [18] developed a strain-rate based permeability model that couples coal deformation and gas flows in both fractures and matrix. The non-uniform deformation of the matrix can be represented by strain-rate for dual-porosity models. However, the time factor is difficult to determine. Chen et al. [28] proposed an interaction coefficient to define the effect of fracture-matrix interactions on porosity evolution. Liu et al. [29] comprehensively discussed the internal swelling coefficient to quantify the contribution of adsorption-induced matrix deformation to fracture aperture and coal permeability. The interaction coefficient was assumed to have an exponential relation with pore pressure difference based on the concept of local swelling [22]. Wei et al. [30] also conducted an experiment to demonstrate the full course of permeability changes evident during matrix swelling.

Although the internal interactions between matrix and fracture have a significant influence on permeability evolution, modeling of this behavior is still a challenging issue. Traditional dual-porosity approaches are computationally much less expensive but more approximate, neglecting the true spatial variation of the gas pressure in the matrix. This approach is accurate only for conventional reservoirs with fewer contrasting properties of matrix and fractures. The MINC approach using a sub-grid can capture the spatial variation of pore pressure in the matrix, but is computationally more expensive. And, as clear from the discussion above, the variation of deformation within matrix blocks is generally neglected in dual porosity/permeability models, together with its transient equilibration without time lag. Thus, the currently available coal-permeability models suffer from the following limitations. They do not consider the interaction between fractures and coal matrix during coal deformation, while this interaction can have a significant effect on permeability changes. For the purpose of successfully prediction of permeability, it becomes necessary to capture the whole process of non-uniformity of the matrix block deformation. To overcome the limitation of dual-porosity approaches, an improved dual-permeability method enlightened by the MINC concept is presented. The matrix block is divided into two sub-blocks utilizing the MINC concept. The mechanical interaction between fracture and matrix is investigated. A sub-matrix permeability model coupling the effect of the effective stress interaction is developed. Based on this conceptual model, we have evaluated this effect on the permeability evolution during CBM extraction.

2. Modelling

2.1. Effect of equilibration time lag between matrix and fracture

In order to describe the pore structure in coal, the dual-porosity model considers an idealized case comprised of a set of identical rectangular parallelepipeds, representing the matrix blocks, which are separated by fractures. Traditional dual-porosity representations are shown useful in modeling large-scale flow through naturally fractured systems. However, there are a number of approximations commonly used in these models that are not always appropriate. The basic assumption is that the pressure is assumed spatially constant within the matrix – or represented as a constant gradient between matrix center and fracture. This assumption is justified when spatial variations of pressure and saturation in the matrix are small, but in other cases, this will lead to inaccuracy [31]. This approach neglects spatial variation within local matrix regions. Actually, the pore pressure within matrix block changes in space. For unconventional reservoirs, gas migration in the matrix can last for months due to the low permeability. There exists an equilibration time lag between matrix and fractures. Thus, the pore pressure drops with increasing distance to fractures as shown in Fig. 1. In addition, the pore pressure is always lower in fractures than the matrix at the same time due to the higher permeability of fracture. Adjacent to the fracture, the variation of pore pressure can be considered as a function of time and space. It is clear that the conventional dual-porosity model fails to capture the actual distribution of gas pressure within the matrix.

The variation of pore pressure strongly affects the effective stress that is a controlling factor in determining the permeability evolution. According to the dual-porosity model, the deformation is uniform for the basic cell under the condition of constant confining stress. This condition is generally met in most conventional reservoirs, but it is not met in low-permeability unconventional reservoirs. The spatial mismatch of deformation in matrix blocks caused by the non-uniform distribution of pore pressure is generally neglected. Therefore, the predicted permeability based on dual-porosity models increases with an increase in gas pressure. By comparison, experimental observations are not able to fit permeability models based on the dual-porosity approach [32]. In fact, the permeability declines with an increase in gas pressure at low gas pressures, then rebounds above the initial value with increasing gas pressure. This is caused by the non-uniform deformation of the matrix

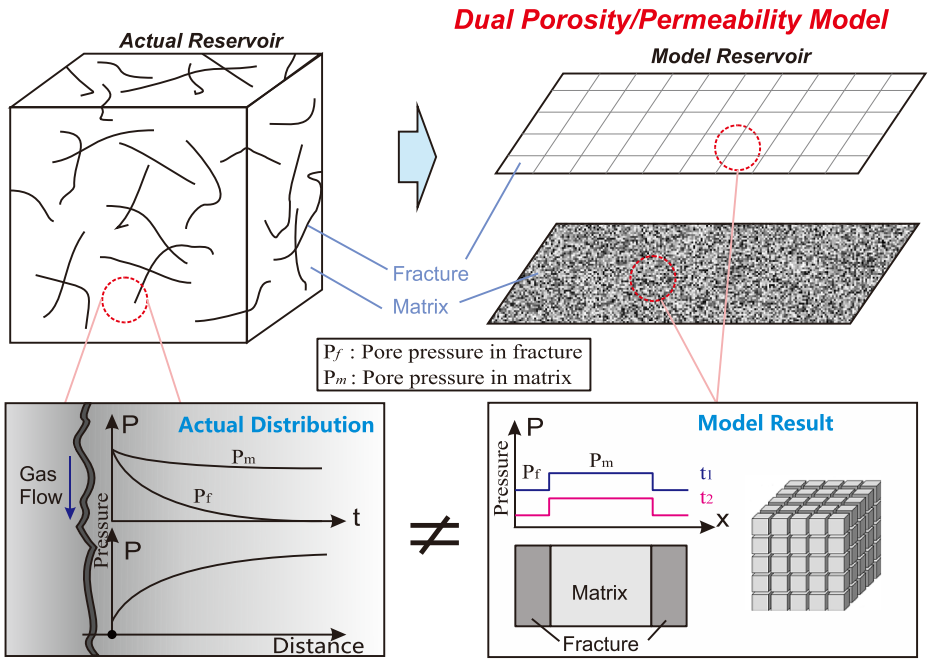

Fig. 1. Schematic of the inconsistency between actual distribution and dual-porosity model results for gas pressure.

induced by the inhomogeneous pore pressure that is neglected in conventional dual-porosity models. Actually, accompanying gas transport, a swelling zone first forms in the area adjacent to the fracture before later propagating throughout the matrix. The non-uniform deformation of the matrix also results in the compression of low density fractures. This can explain why the measured permeability decreases with increasing pore pressure. With an increase in the swelling deformation, the entire sample then swells, resulting in a slow permeability increase. This mechanical interaction leads to significant variation in permeability for low-permeability reservoirs. Thus, these inconsistencies between experimental data and model predictions can be attributed to the spatial variations of matrix strain. The impact of the spatial mismatch between matrix and fracture is unable to be captured in traditional dual-porosity models. Since the swelling deformation is a time-dependent process, a dual-porosity model based on the assumption of uniform swelling is inconsistent with the real physical process. A new model is needed to characterize the effect of the spatial distribution of matrix strain.

2.2. A fully coupled model with equilibration time lag effects

A dual-permeability model allows mass exchange between neighboring matrix blocks while a dual-porosity model does not. In general, gas transfer within the fracture and matrix are assumed to follow Darcy's law. For the case of methane gas, the governing equations for matrix and fracture are established as [18]:

$$\frac{\mathrm{d}}{\mathrm{d}t}\left(\phi_m p_m \frac{\mathrm{M}}{\mathrm{RT}} + (1-\phi_m)\rho_s \rho_{\mathrm{a}} \frac{L_a p_m}{p_m + L_b}\right) - \nabla\left(\rho_{\mathrm{g}} \frac{k_m}{\mu} \nabla p_m\right) = -a_{mf} D_{mf} (\rho_{\mathrm{m}} - \rho_f) \quad (1)$$

$$\frac{\mathrm{d}}{\mathrm{d}t}\left(\phi_f p_f \frac{\mathrm{M}}{\mathrm{RT}}\right) - \nabla(\rho_{\mathrm{g}} \frac{k_f}{\mu} \nabla p_f) = a_{mf} D_{mf} (\rho_{\mathrm{m}} - \rho_f) \quad (2)$$

where ϕ_m and ϕ_f are the porosity of the matrix and fracture system, respectively, p_m and p_f are the gas pressures in matrix and fracture systems, M is the molecular mass of gas, R is the universal gas constant, T is the absolute gas temperature, ρ_{s} is the coal density, ρ_{a} is gas density at atmospheric pressure, L_a is the Langmuir volume constant, L_b is the Langmuir pressure constant, ρ_g is the gas density, k_{m} and k_f are the permeability of matrix and fracture systems, a_{mf} is the shape factor, and D_{mf} is the diffusion coefficient.

As discussed above, the actual deformation of the matrix block is not considered in full detail in the evaluation of the dual-porosity model. The implicit assumption of uniform state variables (pore pressure and matrix properties) is one of the key factors contributing to the mismatch between dual-porosity models and actual response [14]. The MINC model, one of the matrix sub-domain methods, can overcome these limiting assumptions. In this section, the simplest MINC geometry is utilized to characterize the detail of mechanical interaction between fracture and matrix induced by the deformation that accompanies adsorption. It should be noted that the greater the number of matrix cells/nodes, the more accurate the representation of the evolving pressure distribution and strain. However, this comes at a computational cost – so in order to simplify the model, we used a two-part method that captures the essence of the non-uniform pressure distribution at only modest computational cost. Comparing to the dual-porosity model and dual-permeability model, the matrix block is partitioned into two parts M1 and M1′ as shown Fig. 2c.

Based on Eq. (1), only one identical pressure in the matrix can be obtained. In order to realize the description of pressure distribution within the matrix, a sub-matrix is embedded in the center of the matrix blocks as shown in Fig. 2. The solid lines (F1-M1, F2-M2, …) between the fracture and matrix centerlines represent connections where mass exchange is allowed. It illustrates the mass flow both in fracture and insider matrix blocks, as well as fracture-matrix interaction. It can be seen that a dual-permeability model allows matrix-to-matrix flow while a dual-porosity model does not. For the natural fracture, fracture surfaces are generally in contact with each other at some locations, but separated at others. In the sub-matrix model, matrix block M1 is surrounded by fracture F1, as shown in Fig. 2c. The contacted matrix is represented by the sub-matrix M1′. This part of the matrix is not connected with a fracture. So, only matrix block M1 can exchange fluid with the fractures. Due to the fracture-separation, the stress can only transfer through the sub-matrix. A schematic of stress transfer for the sub-matrix concept is shown in Fig. 2d. The volume proportion of sub-matrix in the entire matrix is assumed as A. The matrix blocks are connected though sub-matrix connections as a "bridge". Since the contact area between fracture and matrix is mainly on the surface of M1, the mass exchange between M1' and F1 can be neglected as shown in Fig. 2c. The gas in the

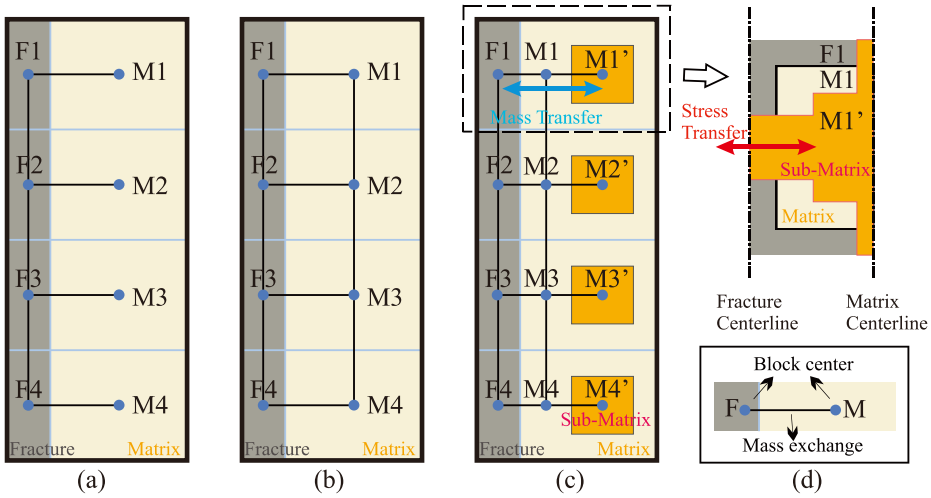

Fig. 2. Schematic of different approaches for conceptualizing fracture-matrix interactions: (a) Flow connection for dual-porosity model; (b) Flow connection for dual-permeability model; and (c) Mass transfer for sub-matrix concept; (d) Stress transfer for sub-matrix concept.

sub-matrix exchanges solely with the matrix. The sub-matrix concept simplifies the gas transport processes within the matrix into two steps: (1) mass exchange between sub-matrix M1' and matrix M1; (2) mass exchange between matrix M1 and fracture F1. The mass governing equation for the sub-matrix can be expressed as:

$$\frac{\mathrm{d}}{\mathrm{d}t}\left(A\phi_m p_m^{'}\frac{\mathrm{M}}{\mathrm{RT}}+A(1-\phi_m)\rho_s\rho_a\frac{L_a p_m^{'}}{p_m^{'}+L_b}\right)-\nabla\left(\rho_g\frac{k_m}{\mu}\nabla p_m^{'}\right)=\frac{1}{\tau}(\rho_m-\rho_m^{'}) \tag{3}$$

where p_m' is gas pressure in the sub-matrix, τ is diffusion time, and A is the volume proportion of the sub-matrix.

Considering the mass exchange from sub-matrix M1′, the governing equation for matrix M1 can be rewritten as:

$$\frac{\mathrm{d}}{\mathrm{d}t}\left(\left(1-A\right)\phi_m p_m\frac{\mathrm{M}}{\mathrm{RT}}+(1-A)(1-\phi_m)\rho_s\rho_a\frac{L_a p_m}{p_m+L_b}\right)-\nabla\left(\rho_g\frac{k_m}{\mu}\nabla p_m\right)$$
$$=-a_{mf}D_{mf}(\rho_m-\rho_f)-\frac{1}{\tau}(\rho_m-\rho_m^{'}) \tag{4}$$

Liu et al. [20] concluded that coal matrix blocks are not completely separated from each other by fractures, in reality. The fracture will be subject to an additional stress during matrix swelling while confining stress remains unchanged. This stress largely results from internal structures (or connectivity of matrix blocks) within the coal. The effective stress for the fractures may be written as:

$$\sigma_f^e=\sigma_t-\alpha p_f+\sigma_f^a \tag{5}$$

where σ_t is the total stress, α is Biot's coefficient, and σ_f^a is additional stress induced by matrix swelling.

Because the coal skeleton is connected by sub-matrix cells, the stress transfer between the sub-matrix cells is shown in Fig. 2d. Thus, the mechanical interaction can be reflected in this conceptual model. Based on this concept, four factors can account for the change in fracture aperture: (1) change of total stress; (2) change of gas pressure in the fracture; (3) deformation in the matrix M1; (4) deformation in the sub-matrix M1′. The change in strain for the fracture is given as:

$$\Delta\varepsilon_f=\Delta\varepsilon_v+\frac{\Delta p_f}{K_f}-\Delta\varepsilon_m+\Delta\varepsilon_{m1} \tag{6}$$

Note that positive values are for matrix swelling and negative ones are for matrix shrinkage. The first part $\Delta\varepsilon_v$ is the increments of volumetric strain due to change in total stress from the external condition. The second part $\Delta p_f/K_f$ is the strain increment due to change in fracture pressure. The third part $\Delta\varepsilon_m$ is the strain increment due to change in matrix strain (M1). The last part $\Delta\varepsilon_{m1}$ is the strain increment due to change sub-matrix strain (M1′). The increase of matrix strain (M1) will result in the decrease in fracture strain. The fracture space is reduced due to squeezing from the swelling matrix. However, the sub-matrix has a positive influence on fracture strain due to the spatial structure of the sub-matrix. The swelling of the sub-matrix will lead to expansion of the whole coal skeleton.

The matrix strain is mainly caused by the adsorption-induced swelling or desorption-induced shrinkage in the coal seam. Adsorption-induced deformation of the coal is one of the key parameters in determining the permeability that influences coal gas extraction. There is an assumption that the volumetric strain of the matrix is proportional to the volume of gas adsorbed. And the amount of gas adsorption is usually related to pressure by the Langmuir equation. Sorption induced volumetric strain can be written as a function of pressure.

Based on previous studies, the fracture permeability can be defined as a function of effective strain [22,27]. As discussed above, fracture deformation is due to three components: external boundary stress, pore pressure, adsorption swelling of the matrix and sub-matrix. Thus, the fracture permeability is established as:

$$\frac{k_f}{k_{f0}}=\left(1+\frac{\alpha}{\phi_{f0}}\left(\Delta\varepsilon_v+\frac{\Delta p_f}{K_f}-\varepsilon_L\frac{p_m}{P_L+p_m}+\varepsilon_L\frac{p_m^{'}}{P_L+p_m^{'}}\right)\right)^3 \tag{7}$$

where ϕ_{f0} and k_{f0} are the initial porosity and permeability of the racture, α is the Biot coefficient, $\Delta\varepsilon_v$ is the volumetric strain, K_f is the bulk modulus of the fracture; ε_L is the Langmuir volumetric strain constant, P_L is the Langmuir pressure constant, and p_m is pore pressure in the matrix.

Assume that the matrix is homogeneous and elastic, and its deformation obeys Hooke's law [33]. The fracture is also assumed homogeneous and elastic with much lower Young's modulus than the matrix. According to the theory of continuum mechanics, the deformation of the coal can be obtained by solving the governing deformation equation [33]. The pore pressure can be calculated by solving Eqs. (2) (3) and (4). Eq. (7) represents the coupling between coal deformation and gas flow. This improved dual-permeability method can fully couple the fracture-matrix interactions. The additional strain from matrix and sub-matrix changes with the distribution of pore pressure within the matrix and asymptotes to zero as the gas pressure equilibrates within the matrix.

3. Model verification

3.1. Variation of coal permeability evolution under constant confining stresses and constant effective stresses

Permeability measurements are typically made shortly after gas pressure reaches preset value. However, experiments on coal deformation find that it may take several months for coal to reach strain equilibrium [34]. Experimental measurements are normally conducted under the assumption of an equilibrium state that necessarily neglects the permeability evolution during the non-equilibrium state. To validate the proposed permeability model, a novel experimental test was conducted [30]. A high volatile bituminous coal sample was collected from Pingdingshan (Henan Province) in China. Coal maceral analyses show that the fractions of vitrinite, semi-vitrinite, liptinite, and inertinite are around 61.7%, 4.5%, 2.9%, and 30.9% respectively. The coal sample was confined under an applied constant boundary stress. Then the upstream boundary of the sample was exposed to CO_2 at fixed gas pressure. Coal permeability was measured continuously throughout the entire period of the experiment from the initial to final equilibrium. The measured permeability changes significantly, as shown in Fig. 3, although the confining pressure and gas pressure were retained constant throughout the experiment. For purposes of comparison, the predicted result from Eq. (7) is also plotted. The parameters used for the model are listed in Table 1. The sources of all parameters are explained in the last column. As indicated in the table, the magnitudes of all selected parameters are consistent with the literatures. Furthermore, no matter what magnitudes we choose for these parameters the permeability would remain as constant when $A = 0$. $A = 0$ represents that the coal deformation is uniform within the matrix. This is the exact solution of conventional dual porosity/permeability models. However, when $A > 0$, the permeability evolves with time. This evolution represents the significant impact of the non-uniform deformation within the matrix. Therefore, it is A, the volumetric fraction of the sub-matrix to the entire matrix, determines the evolution of coal permeability. For this particular experiment, the best value of A to match the experimental observation with the model results is 0.52 as shown in Fig. 3 while the sensitivity of permeability evolution to A is shown in Fig. 4.

Different from traditional permeability tests, this permeability was measured continuously throughout the entire period of the experiment (~80 days). The experimental results show that the permeability increases rapidly due to the decrease in the effective stress within the coal fracture at the beginning of the gas injection. Then, the measured permeability declines from 60 uD to 0.48 uD. It then rebounds slowly for the subsequent two months. As apparent in Fig. 3 the proposed model result is consistent with the experimental data. As the gas is injected into the coal sample, the decrease in the effective stress leads to the instantaneous opening of the fracture following gas injection. After the gas diffuses into the matrix, adsorption-induced swelling deformation occurs in the matrix system, as well. Matrix swelling is primarily localized in the vicinity of the fractures. Simultaneously, the fracture porosity/aperture is reduced in response to the local swelling of the matrix (M1). Thus, it results in a sharp decrease in fracture permeability. With gas flow through the sub-matrix (M1′), the swelling behavior becomes uniform and permeability rebounds due to the swelling of the entire coal block. The influence of mechanical interaction between fracture and matrix on permeability vanishes with the decrease in the pressure differences within the matrix. The time scale of this response depends on the equilibration time lag. It may be concluded that the sub-matrix model fully characterizes the physical process of permeability evolution.

The gas transport properties of the matrix are important in determining permeability evolution. In the new model, two stages of gas transport within the matrix are used to characterize the gas transport

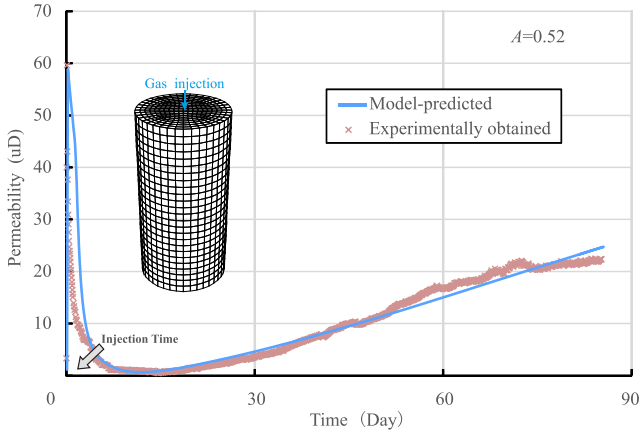

Fig. 3. Comparison between experimental data and predicted permeability during the injection of CO_2.

Table 1
Parameters used in the model.

Parameters	Value	Notes
Young's modulus of the matrix	10 GPa	The selected value is within the range of references: 0.6–6.6 GPa [36] 2.8 GPa [28] 2.9GPa [29] 8.143 GPa [33] 29.1 GPa [28] 22 GPa [23]
Young's modulus of fracture	0.2 GPa	The selected value is consistent with the reference: 0.18 GPa [23]
Langmuir volume, L_a	0.017 m^3/kg	Measured
Langmuir pressure, L_b	4.48 MPa	Measured
Langmuir volumetric strain, ε_L	0.0518	Measured
Shape factor, a_{mf}	12 m^{-2}	12 ~ 60 m^{-2} [37]
Diffusion coefficient, D_{mf}	2×10^{-8} m^2/s	Measured
Diffusion time, τ	4×10^6 s	1×10^6 s [18]
Porosity of matrix, ϕ_m	0.02	The selected value is within the range of references: 0.01, 0.055 [38] 0.038 [39] 0.05 [40]
Porosity of fracture, ϕ_f	0.012	The selected value is consistent with the reference:0.005 [40] 0.012 [39]
Initial permeability of matrix, k_m	2×10^{-18} m^2	The selected value is within the range of references: 1×10^{-18} m^2 [27,33] 2.1×10^{-18} m^2, 9×10^{-18} m^2 [38] 1.47×10^{-19} m^2 [23]
Initial permeability of fracture, k_{f0}	1×10^{-16} m^2	Measured
Temperature, T	20 ℃	Experimental condition
Injection pressure	3 MPa	Experimental condition
Confining stress	6 MPa	Experimental condition
Volume proportion of sub-matrix, A	0.52	0 ~ 1

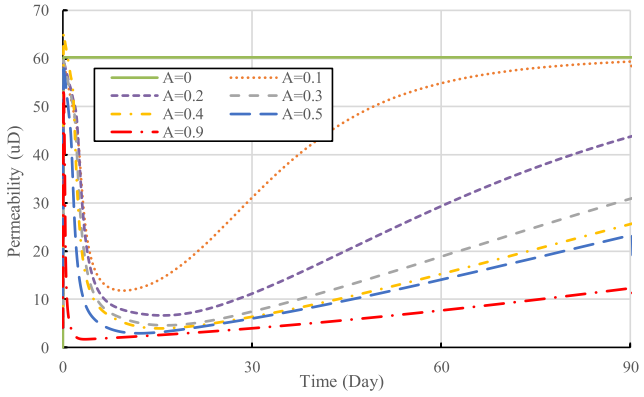

Fig. 4. Effect of volume proportion of sub-matrix on permeability evolution.

processes. The volume proportion of sub-matrix induces an inhomogeneous distribution of pore pressure within the entire matrix block. The effect of volume proportion of sub-matrix on the permeability evolution is shown in Fig. 4. A rebound occurs early when the volume proportion of sub-matrix is small. This indicates that the local swelling induced by the pressure difference vanishes. In contrast, the greater the volume proportion of the sub-matrix, the longer the non-equilibrium between matrix and fracture lasts. Therefore, internal interactions between matrix and fracture suppress the fracture permeability for a long period. One special case is that where the sub-matrix is empty as $A = 0$. The permeability reaches a peak value before remaining constant throughout the later stage. This result indicates that the new model correctly degrades to a conventional dual-permeability model when only matrix and fracture pressures are considered, absent the sub-matrix cells/nodes.

3.2. Variation of coal permeability evolution with change in pore pressure

The model was also evaluated with the experimental data of Robertson [41]. Different component gases, N_2, CH_4 and CO_2, were injected into the specimens. The permeability was measured at different pore pressures. To reveal the mechanisms apparent in the experiments, we conducted three simulations using the sub-matrix model. All the simulations were conducted under the same conditions as the experiments. The parameters used for simulation are chosen from the validation tests and are listed in Table 2.

We compare simulation results with the experimental data by using a vertical bar to represent the variation in permeability with time under the constant injection pressure (Fig. 5). Unlike previous studies, we present coal permeability as a map. A specific point in the map represents the permeability measured under specific pressure and time. It presents the varying range of permeability over time under the constant boundary condition. The height of the vertical bar is highly related to the magnitude of the injection pressure and the gas type. For the case of CO_2, the permeability transits a large range during the gas adsorption process. Permeability variation with N_2 is not as significant compared to the permeability results measured with CO_2. This is attributed to the strong adsorption capacity of CO_2 and confirms that adsorption-induced deformation of the matrix has a strong impact on the fracture permeability. The large strain within the matrix can result in a remarkable spatial mismatch of deformation between fracture and matrix. Compared to model predictions, the experimental data were measured once and under a certain condition. The experimental results can be fitted by choosing appropriate points in the range of model predictions. The solid lines represent the predicted permeability two hours after the initiation of gas injection. It is evident that the selected values of the model result fitted the experimental data well. Therefore, the model prediction is consistent with laboratory observations, although the laboratory data represent permeability only at a given time – and are non-unique.

Table 2
Parameters representing the sample [41].

Parameters	N_2	CH_4	CO_2
Langmuir pressure, L_b	13 MPa	4.26 MPa	3.65 MPa
Langmuir volumetric strain, ε_L	0.00429	0.00777	0.03447
Initial permeability of fracture, k_{f0}	257×10^{-15} m^2	147×10^{-15} m^2	86×10^{-15} m^2
Temperature, T	27 ℃	27 ℃	27 ℃
Confining stress	6.89 MPa	6.89 MPa	6.89 MPa
Volume proportion of sub-matrix, A	0.5	0.5	0.5

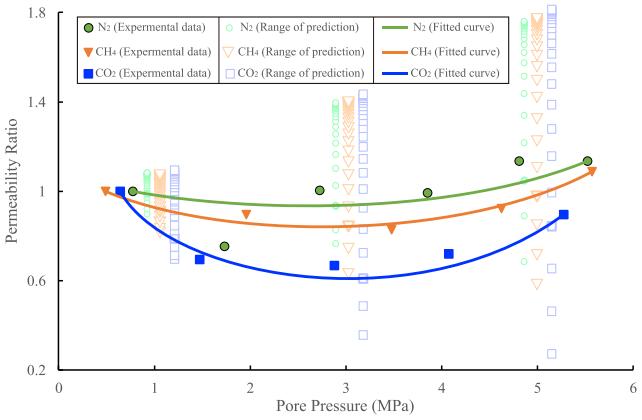

Fig. 5. Comparison of the model-predicted permeability with experimental data under different pore pressures.

4. Results and discussion

4.1. Impact of mechanical interaction on CBM production

As discussed above, the spatial mismatch between fracture and matrix has a significant influence on permeability change. In order to investigate the impact of this mechanical interaction on CBM production, a numerical model representing a coal reservoir is established. The model geometry is 500 m × 500 m with one producing well located in the center of the reservoir. The bottom-hole pressure of the well is set constant. The boundaries of the model are constrained by constant stress with no-flow boundary conditions. The governing equations for mass conservation and deformation-momentum have been imported into the COMSOL Multiphysics platform to solve the partial differential equations. All parameters used for simulation are listed in Table 3.

An effective-strain based permeability model reported by Zhang et al. [17] was used for comparison. This model incorporates the influences of effective stresses and sorption-based volume changes. However, it ignores the influence of mechanical interaction between fracture and matrix. In this study, simulation results with these two models are as shown in Fig. 6. There are distinct differences between the two model results. The gas rate drops sharply after gas production for Zhang's model. A few months later, the gas rate declines steadily. This is because the permeability decreases with a drop in pore pressure, according to Zhang's model. Thus, the gas rate declines with a decrease in

Table 3
Material parameters for field simulation [42,43].

Field parameters	Values	Units
Reservoir depth	500	m
Reservoir thickness	5	m
Reservoir area	500 × 500	m^2
Initial reservoir pressure	4	MPa
Well pressure	0.3	MPa
Coal density	1500	kg/m^3
Young's modulus of matrix	10	GPa
Young's modulus of fracture	0.2	GPa
Langmuir volume, L_a	0.017	m^3/kg
Langmuir pressure, L_b	4.48	MPa
Langmuir volumetric strain, ε_L	0.01	–
Shape factor, a_{mf}	12	m^{-2}
Bulk modulus of the fracture, K_f	0.5	GPa
Diffusion coefficient, D_{mf}	2×10^{-9}	m^2/s
Diffusion time, τ	50	d
Porosity of matrix, ϕ_m	2	%
Porosity of fracture, ϕ_f	1.2	%
Initial permeability of matrix, k_m	2×10^{-18}	m^2
Initial permeability of fracture, k_{f0}	1×10^{-15}	m^2
Temperature, T	45	℃

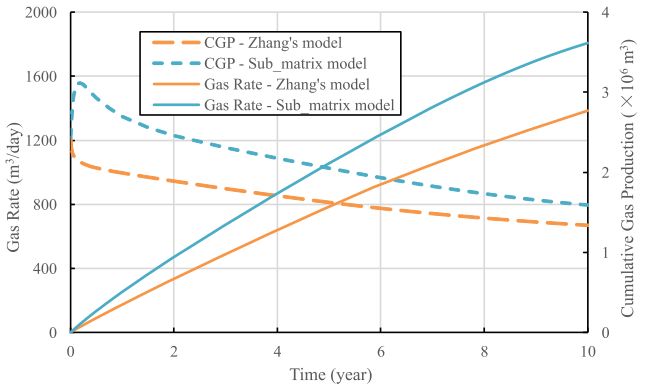

Fig. 6. Flow rate and cumulative gas production (CGP) for different models.

the pore pressure during gas production. For comparison, the new permeability model involves the mechanical interaction from shrinkage of sub-matrix. The evolution of coal permeability is determined by the competing effects of the effective strain and differential strain between matrix and fracture. The result shows that gas rate reaches a peak in the first month before slowly falling with time then finally becoming smooth. As we observe, the difference between the two curves reduces with time. This is because the permeability is dominated by mechanical interaction due to the high-pressure difference in the initial stage according to the new model. As the gas production continues, the pressure difference within the matrix decreases with time. The difference in shrinkage strain between sub-matrix and matrix continues to reduce. It leads to the weakening of the mechanical interaction. At this stage, the permeability is mainly controlled by increasing effective stress. So the dominant factor is the effect of mechanical interaction at the early stage before this switches to the effect of effective stress when the pressure is low. Because the permeability is underestimated by Zhang's model, the predicted cumulative gas production (CGP) is less than that of the sub-matrix model. After ten years of gas extraction, the cumulative gas production is underestimated by 24%.

Fig. 7 shows the distribution of permeability around the production well. As discussed above, the permeability varies in space and time after the reservoir is depleted. Since the reservoir pressure is relatively low near the well, the permeability is much lower than the initial value due to the high effective stress. Further from the wellbore, the effect of pressure depletion on permeability decreases. It can also be seen from Fig. 8 that the formation pressure tends to decline with continuing gas production. The permeability decreases with increased pressure depletion. Significant differences exist in the simulation results both with and without considering the mechanical interaction. The permeability predicted by the sub-matrix model is much greater near the well. This results from the high difference in pressure within the matrix. Long-

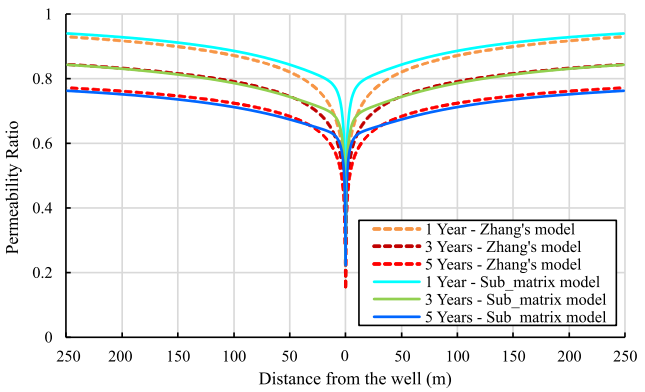

Fig. 7. Permeability distribution for different models.

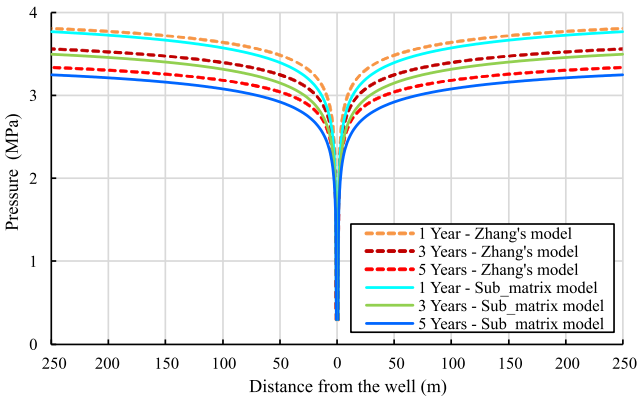

Fig. 8. Pressure distribution for different models.

enduring shrinkage at the edge of the matrix block will result in an increase in fracture porosity/aperture. While shrinkage induced by pressure depletion within the sub-matrix can be ignored at this stage. Therefore, the permeability is enhanced by the non-uniform shrinkage of the matrix. With increasing distance from well, the pressure difference within matrix decreases. Consequently, the gap between the two models reduces for regions far from the well. It could be concluded that neglecting mechanical interaction could introduce significant error in calculation of the permeability and gas production rates.

4.2. *Case study of a soft coal seam*

Fracture stiffness plays an important role in the determination of permeability responding to pressure drawdown. Soft coal with low fracture stiffness is more sensitive to changes in effective stress. In order to evaluate the effect of mechanical interaction and effective stress on permeability variation, a case study of a soft coal seam is presented. The influence of fracture stiffness on the change of permeability is discussed solely in this section. The pore pressure and permeability at detection point A were analyzed for different bulk moduli of the fracture. Point A is 10 m away from the well. Fig. 9 shows how permeability changes with the depletion of pore pressure at point A for three cases. The solid curves represent the predicted permeability including the effect of interaction. The dashed curves represent the predicted permeability without considering the effect of interaction. There are a number of important differences between these curves. Under the influence of mechanical interaction, the permeability predicted by the sub-matirx model is clearly higher at the same pressure. It can also be seen that the difference is evident when the pressure is less than 3.7 MPa. There also exists a

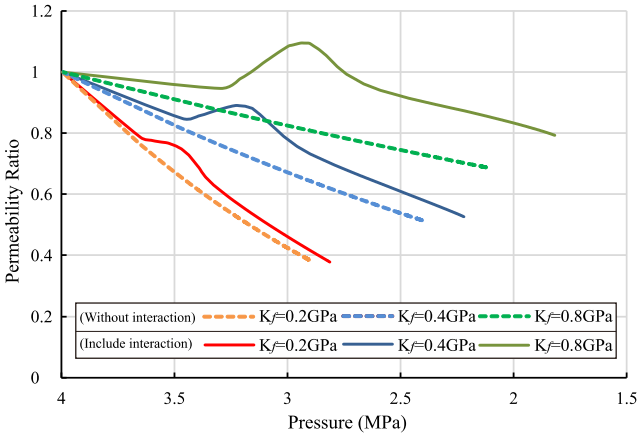

Fig. 9. Variation of permeability with pore pressure for different bulk moduli of the fracture.

pressure range where permeability is greatly enhanced by this effect. This suggests that the pressure gradient is a maximum in this range. The change in permeability caused by mechanical interaction is also linked to the bulk modulus of the fracture. Enhancement of the effect of mechanical interaction increases with the increases in K_f. This suggests that effective stress is a significant contributory factor in the evolution of permeability in soft coal seams. And that the influence of mechanical interaction should be taken into account to avoid the underestimation of gas rate for hard coal seams.

The permeability distribution is shown in Fig. 10 for three cases of different bulk moduli. It is evident that the permeability drops steeply around the well. Away from the well the permeability rises gradually to a background level for all three cases. There is a distinct difference among the three curves. What is interesting in this figure is the peak near the well with a high fracture bulk modulus. Under the influence of mechanical interaction, the permeability is enhanced for the entire region, especially near the well. This is caused by the non-uniform shrinkage deformation within the matrix according to the improved model. A greater deformation difference between matrix and sub-matrix leads to an increase of fracture porosity/aperture. Consequently, the permeability is enhanced markedly around the well. The result show that the permeability of softer coal is much lower after pressure drop. It is consistent with the field experience that permeability would be low in the soft coal seam.

4.3. Case studies of a low-permeability coal seam

It is difficult to extract gas from coal seams with low-permeability. A better understanding of gas flow in low-permeability coal seams can improve gas recovery. The low-permeability of coal is represented by the greater diffusion time in this paper. In order to evaluate the effect of mechanical interaction in low-permeability coal seams, three cases with different diffusion equilibration times were conducted. The longer the diffusion time the greater the equilibration time lag. Fig. 11 shows the variation of permeability with pore pressure for different diffusion times at location A. It appears that the permeability drops only slightly at early time and that this is mainly caused by the decrease in pore pressure. For the case of a diffusion equilibrium time less than 50 days, the difference between the two curves is marginal. When the diffusion equilibrium time is 100 days, the permeability is much higher than for the other two curves. It can also be seen that the difference lasts for a long time. It can be concluded that the influence of mechanical interaction on permeability cannot be ignored, especially for coal seams with low-permeability matrix. The long diffusion time of the matrix can result in a high difference in pressure within the matrix. And this difference can last from early-time production to the end of production. Fig. 12 shows the permeability distribution for different diffusion times after 10 years of gas production. Permeability increases with an increase in the distance to the well for cases with diffusion time less than 50 days. In contrast, the permeability is nearly constant for the case with a diffusion time of 100 days. It is evident that the influence of mechanical interaction is greater near the well. Comparison of results for these three cases indicate that the effects of mechanical interaction endure for a long period for coal seam with low-permeability matrix.

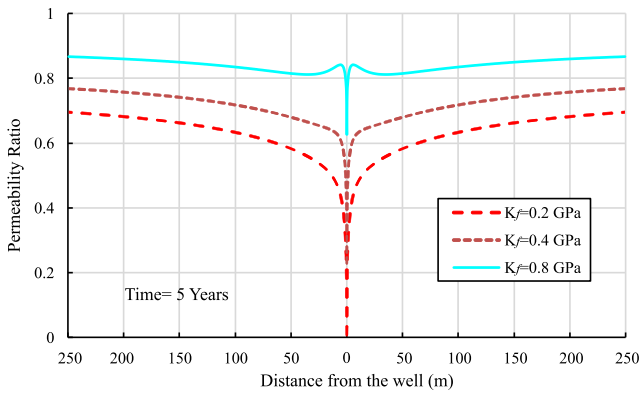

Fig.10. Permeability distribution for different bulk moduli of the fracture.

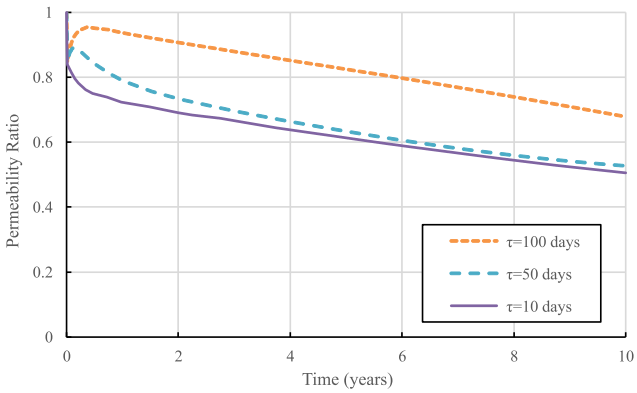

Fig 11. Variation of permeability with pore pressure for different diffusion times.

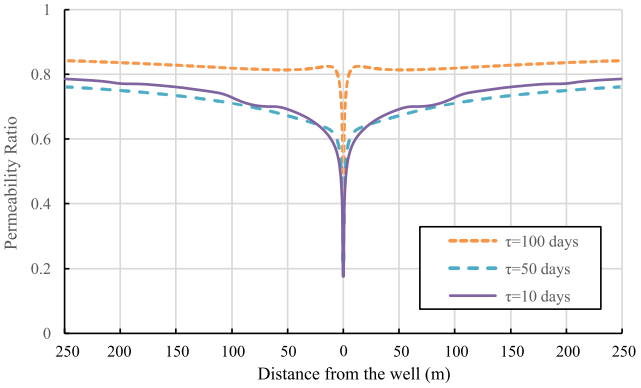

Fig. 12. Permeability distribution for different diffusion times.

5. Conclusions

In this study the conventional dual porosity model is extended to include the impact of equilibration time lag between matrix blocks and fractures. This time lag causes temporal and spatial variations in matrix strain which impact the evolution of fracture permeability. Based on our results, the following conclusions can be drawn:

(1) The evolution of coal permeability is primarily determined by the variation of matrix strain. The matrix strain evolves from initial (zero strain) to ultimate (uniform strain) equilibrium. Conventional dual porosity/permeability models solely represent the two end points (initial and final equilibrium) in this behavior, without the inclusion of matrix-fracture interactions. Our new permeability model correctly accommodates the evolution of coal permeability between these two end points to yield a map of evolving permeabilities.

(2) For low permeability rocks such as coal, the permeability contrast between matrix and fractures is high, resulting in a high equilibration time lag. The time taken for permeability evolution from initial state to ultimate equilibrium state may last from a few days to several tens of years. Therefore, the impact of matrix strain variations on the evolution of coal permeability is significant and should not be ignored.

CRediT authorship contribution statement

Mingyao Wei: Writing - original draft, Methodology. **Jishan Liu:** Conceptualization. **Derek Elsworth:** Writing - review & editing. **Yingke Liu:** Validation. **Jie Zeng:** Writing - review & editing. **Zhihong He:** Investigation.

Declaration of Competing Interest

The authors declare that they have no known competing financial interests or personal relationships that could have appeared to influence the work reported in this paper.

Acknowledgments

This work was supported by the National Key Research and Development Program of China (2020YFA0711802), the Project funded by China Postdoctoral Science Foundation (2019M661997); the National Natural Science Foundation of China (51774277), the Australian Research Council under Grant (DP200101293) and the Science and Technology Major Project of Shanxi Province, China (20201102001). These sources of support are gratefully acknowledged.

References

[1] Fan D, Ettehadtavakkol A. Semi-analytical modeling of shale gas flow through fractal induced fracture networks with microseismic data. Fuel, 2017, 193:444-459.
[2] Warren JE and Root PJ. The Behavior of Naturally Fractured Reservoirs. SPE J. 1963, 3 (3): 245–255. SPE-426-PA.
[3] Kazemi H, Merrill LS, Porterfield JL, Zeman PR. Numerical simulation of water-oil flow in naturally fractured reservoirs. Society of Petroleum Engineers Journal, 1976, 16(6):1114-1122.
[4] Thomas LK, Dixon TN, Pierson RG. Fractured Reservoir Simulation: SPE Journal, 1983, 23(1):42-54.
[5] Saidi A. Simulation of naturally fractured reservoirs. SPE 12270, in Proceedings SPE Reservoir Simulation Symposium, 1983, Society of Petroleum Engineers.
[6] Pruess K, Narasimhan TN. A practical method for modeling fluid and heat flow in fractured porous media. SPE J 1985;25(1):14–26.
[7] Sarma P, Aziz K. New transfer functions for simulation of naturally fractured reservoirs with dual-porosity models. SPE J 2006;11(3):328–40.
[8] Wu YS, Li J, Ding D, Wang C, Di Y. A generalized framework model for the simulation of gas production in unconventional gas reservoirs. SPE J 2014;19(05):845–57.
[9] Cai L, Ding D-Y, Wang C, Wu Y-S. Accurate and efficient simulation of fracture–matrix interaction in shale gas reservoirs. Transp Porous Media 2015;107(2):305–20.
[10] Wang C, Wu YS. Modeling analysis of transient pressure and flow behavior at horizontal wells with multi-stage hydraulic fractures in shale gas reservoirs. Society of Petroleum Engineers. Society of Petroleum Engineers SPE Unconventional Resources Conference - The Woodlands, Texas, USA, 2014-04-01.
[11] Gilman JR. An efficient finite-difference method for simulating phase segregation in the matrix blocks in double-porosity reservoirs. SPE Reservoir Eng 1986;1(4):403–13.
[12] Beckner B, Chan H, McDonald A, Wooten S, Jones T. Simulating naturally fractured reservoirs using a subdomain method, in Proceedings SPE Symposium on Reservoir Simulation, 1991, Society of Petroleum Engineers.
[13] Karimi-Fard M, Gong B, Durlofsky LJ. Generation of coarse-scale continuum flow models from detailed fracture characterizations. Water Resour Res 2006;42(10):1–9.
[14] Elfeel A, Mohamed. Improved upscaling and reservoir simulation of enhanced oil recovery processes in naturally fractured reservoirs. Heriot-Watt University, 2014.
[15] Gray I. Reservoir engineering in coal seams: part 1-the physical process of gas storage and movement in coal seams. SPE Reservoir Eng 1987;2:28–34.
[16] Cui XJ, Bustin RM. Volumetric strain associated with methane desorption and its impact on coalbed gas production from deep coal seams. AAPG Bull 2005;89:1181–202.
[17] Zhang HB, Liu JS, Elsworth D. How sorption-induced matrix deformation affects gas flow in coal seams: a new FE model. Int J Rock Mech Min Sci 2008;45(8):1226–36.
[18] Wei MY, Liu JS, Elsworth D, Li SJ, Zhou FB. Influence of gas adsorption induced non-uniform deformation on the evolution of coal permeability. Int J Rock Mech Min Sci 2019;114:71–8.
[19] Zhou Y, Li Z, Yang Y, Zhang L, Qi Q, Si L, et al. Improved porosity and permeability models with the coal matrix block deformation effect. Rock Mech Rock Eng 2016;49:3687–97.
[20] Liu HH, Rutqvist J. A new coal-permeability model: internal swelling stress and fracture-matrix interaction. Transp Porous Med 2009;82(1):157–71.
[21] Chen Z, Liu J, Pan Z, Connell LD, Elsworth D. Influence of the effective stress coefficient and sorption-induced strain on the evolution of coal permeability: model development and analysis. Int J Greenh Gas Con 2012;8(5):101–10.
[22] Liu JS, Wang JG, Chen ZW, Wang SG, Elsworth D, Jiang YD. Impact of transition from local swelling to macro swelling on the evolution of coal permeability. Int J Coal Geol 2011;88(1):31–40.
[23] Wang G, Wang K, Wang SG, Elsworth D, Jiang YJ. An improved permeability evolution model and its application in fractured sorbing media. J Nat Gas Sci Eng 2018;56:222–32.
[24] Pang Y, Soliman MY, Deng HC, Xie XH. Experimental and analytical investigation of adsorption effects on shale gas transport in organic nanopores. Fuel 2017;199:272–88.
[25] Wu W, Zoback MD, Kohli AH. The impacts of effective stress and CO2, sorption on the matrix permeability of shale reservoir rocks. Fuel 2017;203:179–86.
[26] Lewis R, Pao W. Numerical simulation of three-phase flow in deforming fractured reservoirs. Oil Gas Sci Technol 2002;57:499–514.
[27] Zhang SW, Liu JS, Wei MY, Eslworth D. Coal permeability maps under the influence of multiple coupled processes. Int J Coal Geol 2018;187:71–82.
[28] Chen M, Hosking LJ, Sandford RJ, Thomas HR. Dual porosity modelling of the coupled mechanical response of coal to gas flow and adsorption. Int J Coal Geol 2019;205:115–25.
[29] Liu T, Lin BQ, Yang W. Impact of matrix–fracture interactions on coal permeability: Model development and analysis. Fuel 2017;207:522–32.
[30] Wei MY, Liu JS, Shi R, Elsworth D, Liu ZH. Long-Term evolution of coal permeability under effective stresses gap between matrix and fracture during co2 injection. Transp Porous Media 2019;130(3):969–83.
[31] Gong B, Effective Models of Fractured Systems., 2007, Stanford University, Doctor of philosophy.
[32] Shi R, Liu JS, Wei MY, Elsworth D, Wang XM. Mechanistic analysis of coal permeability evolution data under stress-controlled conditions. Int. J. R. Mech. and Min. Sci., 2018,110:36-47.
[33] Wu Y, Liu JS, Elsworth D, Chen ZW, Connell LD, Pan ZJ. Dual poroelastic response of a coal seam to CO2 injection. Int J Greenhouse Gas Cont 2010;4:668–78.
[34] Danesh NN, Chen Z, Connell LD, Kizil MS, Pan Z, Aminossadati SM. Characterization of creep in coal and its impact on permeability: An experimental study. Int. J. Coal Geol. 2017;173:200–11.
[36] Wang CG, Feng JL, Liu JS, Wei MY, Wang CS, Gong B. Direct observation of coal–gas interactions under thermal and mechanical loadings. Int J Coal Geol 2014;131:274–87.
[37] Ranjbar E, Hassanzadeh H. Matrix–fracture transfer shape factor for modeling flow of a compressible fluid in dual-porosity media. Adv Water Resour 2011;34(5):627–39.
[38] Peng Y, Liu J, Wei M, Pan Z, Connell LD. Why coal permeability changes under free swellings: New insights. Int. J. Coal Geol. 2014;133:35–46.
[39] Si LL, Li ZH, Yang YL, Gao RT. The stage evolution characteristics of gas transport during mine gas extraction: Its application in borehole layout for improving gas production. Fuel 2019;241:164–75.
[40] Wei ZJ, Zhang DX. Coupled fluid-flow and geomechanics for triple-porosity/dual-permeability modeling of coalbed methane recovery. Int J Rock Mech Min Sci 2010;47(8):1242–53.
[41] Robertson EP. Measurement and modeling of sorption-induced strain and permeability changes in coal. PhD dissertation, Colorado School of Mines, Golden, 2005, Colorado.
[42] Aminian K, Ameri S. Predicting production performance of CBM reservoirs. J Nat Gas Sci Eng 2009;1(1–2):25–30.
[43] Zhu HY, Tang XH, Liu QY, Liu SJ, Zhang BH, Jiang S, et al. Permeability stress-sensitivity in 4D flow-geomechanical coupling of Shouyang CBM reservoir, Qinshui Basin. China. Fuel 2018;232:817–32.